doi:10.3772/j.issn.1006-6748.2023.04.003

A novel adaptive temporal-spatial information fusion model based on Dempster-Shafer evidence theory①

HU Zhentao(胡振涛), SU Yujie②, ZHANG Zihan
(School of Artificial Intelligence, Henan University, Zhengzhou 450046, P. R. China)

Abstract

In the field of target recognition based on the temporal-spatial information fusion, evidence theory has received extensive attention. To achieve accurate and efficient target recognition by the evidence theory, an adaptive temporal-spatial information fusion model is proposed. Firstly, an adaptive evaluation correction mechanism is constructed by the evidence distance and Deng entropy, which realizes the credibility discrimination and adaptive correction of the spatial evidence. Secondly, the credibility decay operator is introduced to obtain the dynamic credibility of temporal evidence. Finally, the sequential combination of temporal-spatial evidences is achieved by Shafer's discount criterion and Dempster's combination rule. The simulation results show that the proposed method not only considers the dynamic and sequential characteristics of the temporal-spatial evidences combination, but also has a strong conflict information processing capability, which provides a new reference for the field of temporal-spatial information fusion.

Key words: temporal-spatial information fusion, evidence theory, Deng entropy, evidence distance, credibility decay model

0 Introduction

Dempster-Shafer (DS) evidence theory[1-2], also known as the belief function theory, is essentially a generalization of Bayesian theory[3]. Compared with Bayesian theory, DS evidence theory can effectively achieve the representation and processing of uncertain information without prior knowledge[4]. In addition, DS evidence theory can represent the stochastic uncertainty information, the incomplete information, and the subjective uncertainty information better. Therefore, DS evidence theory can be applied to solve many problems, such as temporal-spatial information fusion.

The temporal-spatial information fusion technology is a combination of temporal and spatial, which can solve the problem of target recognition under complex conditions that is difficult to be satisfied by a single spatial or temporal information fusion technology.

During the development of temporal-spatial information fusion technology, many related temporal fusion methods have been proposed[5-7]. But they all ignored the influence of temporal factors on the fusion results. Therefore, some scholars have determined the discount weight of historical moment fusion information from different perspectives. Song et al.[8] constructed a credibility decay model by analyzing the characteristics of temporal information fusion, which is an effective mean to achieve the temporal information fusion. But it fails to pay attention to the impact of spatial high-conflict information on the temporal-spatial fusion results, which will lead to the deterioration of the anti-interference ability of the model. Although some methods[9-10] existing can compensate for the shortcomings of the credibility decay model to some extent, they still have a lot of room for improvement. In addition, Li et al.[11] constructed an optimization model for solving temporal weights by quantifying the decision maker's preference for the temporal order. But this method needs to be performed after certain moments accumulation, which does not reflect the real-time characteristic of temporal information fusion. Refs[12,13] performed the assignment of temporal weights by the ordered weighted aggregation (OWA) operator and the visibility graph averaging (VGA). However, the method only focuses on the order of time nodes and ignores the impact that his-

① Supported by the National Natural Science Foundation of China (No. 61976080), the Key Project on Research and Practice of Henan University Graduate Education and Teaching Reform (YJSJG2023XJ006), the Key Research and Development Projects of Henan Province (231111212500), the Henan University Graduate Education Innovation and Quality Improvement Program (SYLKC2023016).

② To whom correspondence should be addressed. E-mail: syjxxn@henu.edu.cn.

Received on Feb, 21, 2023

torical information brings to the current moment.

To solve the above problems, this paper proposes an adaptive temporal-spatial information fusion method based on the DS evidence theory, which mainly includes two steps. Firstly, the spatial fusion method based on Deng entropy and evidence distance is established. By considering the correlation between evidences and the information volume of the credible evidence, the conflicting information among the spatial evidences can be effectively processed and a reasonable spatial fusion result can be produced. Secondly, based on the credibility decay model and Shafer's discount criterion, the historical cumulative fusion information is discounted, which is combined with the spatial fusion result at the current moment by Dempster's combination rule. This method can obtain atemporal-spatial fusion result with high accuracy because it follows the sequential nature of the temporal information fusion.

The other sections of this paper are organized as follows. Section 1 introduces some basic concepts. Section 2 proposes an adaptive temporal-spatial information fusion model based on the DS evidence theory. Section 3 discusses the rationality and superiority of the proposed method through a simulation. Section 4 summarizes this paper.

1 Preliminary

1.1 DS evidence theory

If there is a set $\Theta = \{\theta_1, \theta_2, \theta_3, \cdots, \theta_u\}$ that consists of u mutually exclusive elements, then Θ is called the frame of discernment (FOD). The power set of Θ constitutes a set containing 2^{Θ} elements, denoted as $2^{\Theta} = \{\theta_1, \theta_2, \cdots, \theta_u, \theta_1 \cup \theta_2, \cdots, \Theta, \phi\}$.

For $A \in 2^{\Theta}$, if the mapping $m: 2^{\Theta} \to [0,1]$ satisfies the following conditions.

$$m(\phi) = 0 \tag{1}$$

$$\sum_{A \in 2^{\Theta}} m(A) = 1 \tag{2}$$

where, m is called a basic probability assignment (BPA). $m(A)$ is the belief value assigned to the proposition A. When $m(A) > 0$, A is the focal element of m. The vector form of m is denoted as $\boldsymbol{m}$.

Assuming that two different BPAs m_1 and m_2; $A_1, A_2, \cdots, A_k$ and $B_1, B_2, \cdots, B_l$ represent the focal elements of m_1 and m_2, respectively. The combined BPA is denoted by m. Then, Dempster's combination rule is denoted as

$$m(A) = \begin{cases} 0 & A = \Phi \\ \dfrac{\sum_{A_p \cap B_q = A} m_1(A_p) m_2(B_q)}{1 - K} & A \neq \Phi \end{cases} \tag{3}$$

where, $K = \sum_{A_p \cap B_q = \Phi} m_1(A_p) m_2(B_q)$ $(p = 1, 2, \cdots, k;\ q = 1, 2, \cdots, l)$ is the conflict coefficient representing the degree of conflict between evidences. The larger the value of K, the greater the degree of conflict between evidences.

Assuming that $m(A)$ is a BPA defined on Θ, the Pignistic probability transformation $BetP_m: 2^{\Theta} \to [0,1]$ is denoted as

$$BetP_m(\theta_r) = \sum_{A \subseteq \Theta, \theta_r \in A} \frac{m(A)}{|A|} \tag{4}$$

where, $|A|$ is the cardinality of the set A.

1.2 Evidence distance

Peng et al.[14] proposed a method to measure the distance between BPA functions. Let $\boldsymbol{m}_1$ and $\boldsymbol{m}_2$ be vector forms of BPAs m_1 and m_2 in the same frame of discernment. Then the distance between m_1 and m_2 can be defined as

$$md_{\mathrm{BPA}}(m_1, m_2) = \sqrt{\frac{(\boldsymbol{m}_1, \boldsymbol{m}_1) + (\boldsymbol{m}_2, \boldsymbol{m}_2) - 2(\boldsymbol{m}_1, \boldsymbol{m}_2)}{(\boldsymbol{m}_1, \boldsymbol{m}_1) + (\boldsymbol{m}_2, \boldsymbol{m}_2)}} \tag{5}$$

The greater the distance between evidences, the greater the difference between evidences.

1.3 Uncertainty measure

To measure the uncertainty of BPA, some scholars introduced the Shannon entropy. Based on the Shannon entropy, Ref. [15] proposed the Deng entropy, defined as

$$E_d(m) = -\sum_{A \subseteq \Theta} m(A) \log_2 \frac{m(A)}{2^{|A|} - 1} \tag{6}$$

1.4 Credibility decay model

For the sequential character of the temporal information fusion, Ref. [8] created a credibility decay model by combining the Markovian property with the evidence discount theory. Let $\{(t_1, m_1), (t_2, m_2), \cdots, (t_n, m_n)\}$ be the BPAs of n evidences obtained from time nodes $t_1, \cdots, t_i, \cdots, t_n$ and g be the Dempster's combination rule. The dynamic combination result $f_n(m_1, m_2, \cdots, m_n)$ of n evidences using the credibility decay model can be denoted as

$$f_n(m_1, m_2, \cdots, m_n) = g(\cdots(g(m_1^{\alpha(1,2)}, m_2)^{\alpha(2,3)}, \cdots, m_{n-1})^{\alpha(n-1,n)} m_n) \tag{7}$$

where, t_n and m_n are the time point at which evidence is collected and the BPA at that moment, respectively. The dynamic credibility α at t_i of the BPA m_j obtained at t_j is defined as

$$\begin{cases} \alpha_{ij} = \mathrm{e}^{-\lambda(t_i, t_j)} \\ \lambda \in [0, \ln 2] \end{cases} \tag{8}$$

2 The proposed adaptive temporal-spatial information fusion model

With the increasing complexity of the target recognition scenarios, the recognition information obtained by a single sensor at a single moment is often not accurate. To ensure the target recognition accuracy, the temporal-spatial fusion of the recognition information is often required. Therefore, a new adaptive temporal-spatial information fusion model is proposed. The specific process is shown in Fig. 1.

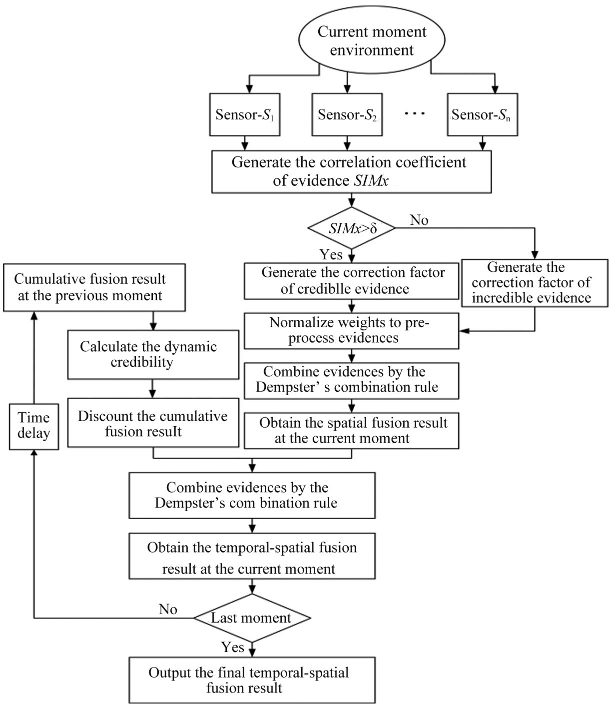

Fig. 1 Temporal-spatial fusion method based on adaptive processing strategy

2.1 Support coefficient of the spatial evidence

Assume the multi-sensor system has n heterogeneous sensors: $S_1, S_2, \cdots, S_x, \cdots, S_n (x = 1, 2, \cdots, n)$. Multiple sensors perform target recognition at t_i and the recognition information is converted into the BPAs m_i^1, $m_i^2, \cdots, m_i^x, \cdots, m_i^n$, where m_i^x is the BPA obtained by the sensor S_x at t_i.

Step 1 For the updated information sequence $m_i^1, m_i^2, \cdots, m_i^x, \cdots, m_i^y, \cdots, m_i^n$ acquired by n sensors at t_i, they are viewed as n spatial evidences. The degree of correlation between the spatial evidences is obtained by

$$rel(m_i^x, m_i^y) = 1 - md_{BPA}(m_i^x, m_i^y) \tag{9}$$

where $rel(m_i^x, m_i^y)(x, y = 1, 2, \cdots, n)$ represents the similarity between m_i^x and m_i^y.

Step 2 The similarity matrix is represented as

$$\boldsymbol{RC} = \begin{bmatrix} 1 & \cdots & \mathrm{rel}(\mathrm{m_i^1}, \mathrm{m_i^n}) \\ \vdots & \ddots & \vdots \\ \mathrm{rel}(\mathrm{m_i^n}, \mathrm{m_i^1}) & \cdots & 1 \end{bmatrix} \tag{10}$$

Step 3 The support coefficient Sup_x of the spatial evidence is expressed as

$$Sup_x = \sum\nolimits_{y=1, x \neq y}^{n} rel(m_i^x, m_i^y) \tag{11}$$

Step 4 The correlation coefficient SIM_x of the spatial evidence is defined as

$$SIM_x = \frac{Sup_x}{\sum\nolimits_{x=1}^{n} Sup_x} \tag{12}$$

Step 5 Set the threshold δ. And distinguish the credible evidence from the incredible evidence based on the support coefficient Sup_x of the evidence and the threshold δ.

$$\delta = \sum\nolimits_{x=1}^{n} \varphi \times Sup_x \tag{13}$$

If $Sup_x > \delta$, the evidence m_i^x is credible. Otherwise, it is incredible.

2.2 Correction factor of the spatial evidence

Step 1 For the credible evidence, the information volume is introduced to obtain its correction factor:

$$CF_x = \left(1 - \frac{E_d(m_i^x)}{\log_2 10}\right) \mathrm{e}^{-\frac{E_d(m_i^x)}{\log_2 10}} \tag{14}$$

Step 2 For the incredible evidence, its evidential correlation coefficient SIM_x is regarded as the correction factor. The normalized correction factor is denoted as

$$w_x = \frac{CF_x}{\sum\nolimits_{x=1}^{n} CF_x} \tag{15}$$

Step 3 Weight the spatial evidences according to the normalized correction factor w_x and generate the pre-processed BPA function m_i':

$$m_i'(A) = \sum\nolimits_{x=1}^{n} w_x \times m_i^x(A) \tag{16}$$

Step 4 The pre-processed evidence m_i' is fused $(n-1)$ times by Dempster's combination rule to obtain the multi-sensor spatial fusion result m_i at t_i.

2.3 Temporal-spatial evidences fusion

Assume $\oplus m_1, \oplus m_2, \cdots, \oplus m_{i-1}$ are the cumulative fusion information at the historical moments $t_1, t_2, \cdots, t_{i-1}$, respectively.

Step 1 On entering the next moment t_i, the credibility factor α of the cumulative fusion result

$\oplus m_{i-1}$ at t_i can be calculated by Eq. (8).

Step 2 The cumulative fusion result $\oplus m_{i-1}$ is discounted by Shafer's discounting criterion

$$m_{i-1}^{\alpha}(A) = \begin{cases} \alpha m_{i-1}(A) & A \neq \Theta \\ 1 - \alpha + \alpha m_{i-1}(A) & A = \Theta \end{cases} \quad (17)$$

Step 3 Combine the discounted result $\oplus m_{i-1}^{\alpha}$ and the temporal update evidence m_i at t_i by the Dempster's combination rule. The final result is the cumulative fusion evidence $\oplus m_i$ at t_i.

3 Simulation results and analysis

The example presented in Ref. [16] is applied to verify the feasibility and effectiveness of the proposed adaptive temporal-spatial information fusion method in this paper. In this simulation, λ is taken as 0.05 and φ is taken as 0.143.

In this simulation, there are six heterogeneous sensors S_1, S_2, S_3, S_4, S_5 and S_6, which are assigned to collect the target recognition information at each time point. The collected target recognition information is independent of each other and is transformed into the BPAs. There is a frame of discernment constructed from the targets θ_1 (Bullet), θ_2 (Balloon) and θ_3 (Fragment), denoted as $\Theta = \{\theta_1, \theta_2, \theta_3\}$. And the BPAs for target recognition formed by multiple sensors at different moments can be seen in Table 1.

3.1 Spatial evidences combination

From Table 1, the presence of the sensor S_5 leads to a large conflict among evidences at t_1. But the sensors S_1, S_2, S_3, S_4, S_6 all give larger support to the target $\{\theta_3\}$ at t_1. Therefore, the result of target recognition should be the target $\{\theta_3\}$. Obviously, from t_2 to t_5, there is a low conflict among spatial evidences.

Table 1 BPA for target recognition formed by different sensors at each time node

Time point/s	BPA						
	BPM	S_1	S_2	S_3	S_4	S_5	S_6
$t_1 = 5$	$m(\{\theta_1\})$	0.2500	0.3000	0.2210	0.3330	0.6290	0.3050
	$m(\{\theta_2\})$	0.2990	0.2560	0.3500	0.2730	0.3520	0.2120
	$m(\{\theta_3\})$	0.4510	0.4440	0.4290	0.3940	0.0190	0.4830
$t_2 = 8$	$m(\{\theta_1\})$	0.4400	0.6280	0.4350	0.3480	0.6420	0.5300
	$m(\{\theta_2\})$	0.3230	0.1360	0.3250	0.2620	0.2520	0.1180
	$m(\{\theta_3\})$	0.2370	0.2360	0.2400	0.3900	0.1060	0.3520
$t_3 = 16$	$m(\{\theta_1\})$	0.2510	0.4540	0.2690	0.4600	0.6230	0.1240
	$m(\{\theta_2\})$	0.2760	0.2360	0.3360	0.2150	0.1420	0.4200
	$m(\{\theta_3\})$	0.4730	0.3100	0.3950	0.3250	0.2350	0.4560
$t_4 = 23$	$m(\{\theta_1\})$	0.3370	0.3180	0.2620	0.2460	0.4350	0.3120
	$m(\{\theta_2\})$	0.3030	0.2690	0.2030	0.2620	0.2590	0.3420
	$m(\{\theta_3\})$	0.3600	0.4130	0.5350	0.4920	0.3060	0.3460
$t_5 = 26$	$m(\{\theta_1\})$	0.3360	0.3460	0.2410	0.3680	0.3300	0.3030
	$m(\{\theta_2\})$	0.3120	0.3050	0.2580	0.2620	0.3010	003910
	$m(\{\theta_3\})$	0.3520	0.6490	0.5010	0.3700	0.3690	0.3060

The spatial fusion results of the BPAs in Table 1 obtained by the Dempster's combination method, the method in Ref. [16], and the proposed method are shown in Table 2, Table 3, and Table 4, respectively. The spatial fusion results show that all three methods can obtain fusion results consistent with the intuitive analysis from t_2 to t_5. Because there is a low conflict among spatial evidences from t_2 to t_5. In comparison, it is found that the support for the target obtained by the proposed method is higher. However, if there is a large conflict, such as the sensor S_5 at t_1, the Dempster's method generates the wrong recognition result $\{\theta_1\}$. The method in Ref. [16] and the proposed method both give high support for the target $\{\theta_3\}$, which demonstrates the ability of the proposed method to handle the conflict existing in spatial information.

3.2 Temporal-spatial evidences combination

According to the spatial fusion results, BPA at every moment except t_2 has greater support for the target $\{\theta_3\}$. Therefore, the final identification result should be the target $\{\theta_3\}$. For comparison and analysis, the

Table 2 Spatial fusion results obtained by Dempster's combination rule

Time point/s	$m(\{\theta_1\})$	$m(\{\theta_2\})$	$m(\{\theta_3\})$
$t_1 = 5$	0.5529	0.2850	0.1621
$t_2 = 8$	0.9489	0.0377	0.0134
$t_3 = 16$	0.3216	0.0829	0.5955
$t_4 = 23$	0.1715	0.0703	0.7582
$t_5 = 26$	0.2365	0.1737	0.5898

Table 3 Spatial fusion results obtained by the method in Ref. [16]

Time point/s	$m(\{\theta_1\})$	$m(\{\theta_2\})$	$m(\{\theta_3\})$
$t_1 = 5$	0.2322	0.1299	0.6379
$t_2 = 8$	0.9509	0.0189	0.0302
$t_3 = 16$	0.4425	0.0993	0.4582
$t_4 = 23$	0.1951	0.0920	0.7129
$t_5 = 26$	0.2546	0.1956	0.5498

Table 4 Spatial fusion results obtained by the proposed method

Time point/s	$m(\{\theta_1\})$	$m(\{\theta_2\})$	$m(\{\theta_3\})$
$t_1 = 5$	0.1017	0.0728	0.8265
$t_2 = 8$	0.9775	0.0077	0.0145
$t_3 = 16$	0.2412	0.1094	0.6494
$t_4 = 23$	0.1628	0.0639	0.7733
$t_5 = 26$	0.2415	0.1668	0.5917

temporal-spatial cumulative fusion results obtained by different methods at each moment are given in Table 5. From Table 5, it can be seen that, due to the system perturbation at t_2, the cumulative fusion results obtained by different methods give higher support for the incorrect target $\{\theta_1\}$ than the correct target $\{\theta_3\}$. And starting from t_3, the recognition system recovers from the perturbation and the support for the target $\{\theta_3\}$ by each method is improved. In contrast, the proposed method can recover from the disturbance state too quickly and generate the highest recognition accuracy at t_5, because it takes into account the adaptive correction of spatial evidences as well as the credibility decay of historical evidences.

The trends of the Pignistic probabilities over time obtained by Dempster's method, the method in Ref. [8], the method in Ref. [16], the method in Ref. [12], and the proposed method are shown in Fig. 2 to Fig. 6, respectively. In Fig. 6, there is the $BetP_m(\theta_3) > BetP_m(\theta_1) > BetP_m(\theta_2)$, except at t_2 when there is a strong perturbation. And the support of the proposed method for the target $\{\theta_3\}$ is significantly greater than the target $\{\theta_1\}$ at t_3. This indicates that the proposed method can converge faster and focus on the correct target faster when the sensors recover from the perturbation.

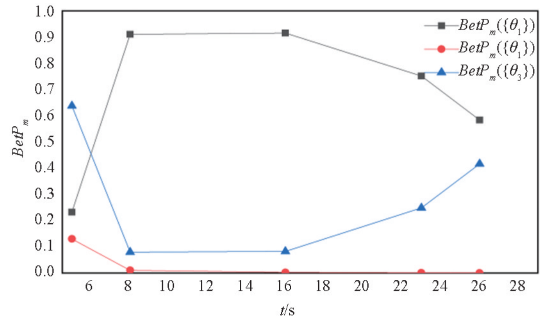

Fig. 2 Temporal-spatial fusion results obtained by Dempster'smethod at each moment

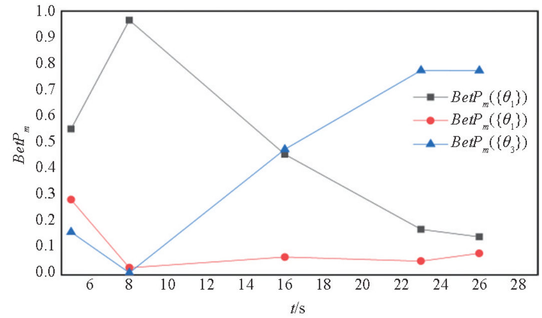

Fig. 3 Temporal-spatial fusion results obtained by the method in Ref. [8] at each moment

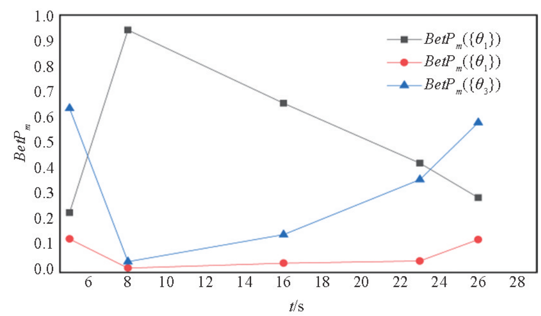

Fig. 4 Temporal-spatial fusion results obtained by the method in Ref. [16] at each moment

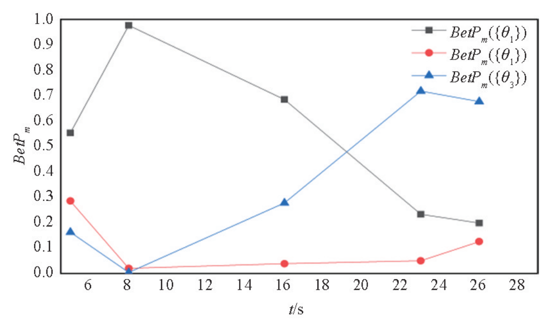

Fig. 5 Temporal-spatial fusion results obtained by the method in Ref. [12] at each moment

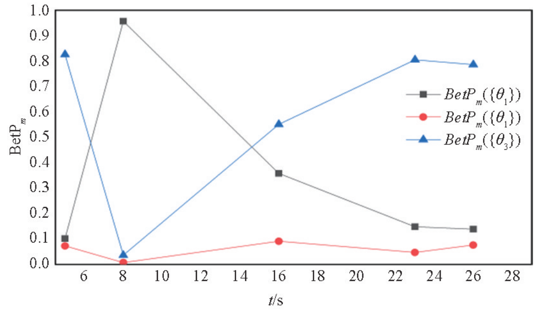

Fig. 6 Temporal-spatial fusion results obtained by the proposed method at each moment

4 Conclusions

In order to realize the target recognition based on the temporal-spatial information fusion, an adaptive temporal-spatial information fusion method is proposed in this paper. Firstly, the evidence distance and the Deng entropy are introduced to measure and correct spatial evidence, thus generating the updated evidence at the current moment. Secondly, combined with the credibility decay model, the historical cumulative fusion evidence from the previous moment is discounted in the temporal system. Finally, the temporal-spatial information fusion is achieved by combining discounted historical evidence with updated evidence. The simulation results show that the proposed adaptive temporal-spatial information fusion method is based on the characteristics of information inheritance and can update in temporal information fusion. In addition, the method has strong anti-interference ability.

Table 5 Temporal-spatial fusion results of different methods

Method	Temporal-spatial fusion results				
	t_1 = 5	t_2 = 8	t_3 = 16	t_4 = 23	t_5 = 26
Dempster[1]	$m(\{\theta_1\})$ = 0.2322	$m(\{\theta_1\})$ = 0.9105	$m(\{\theta_1\})$ = 0.9150	$m(\{\theta_1\})$ = 0.7512	$m(\{\theta_1\})$ = 0.5835
	$m(\{\theta_2\})$ = 0.1299	$m(\{\theta_2\})$ = 0.0101	$m(\{\theta_2\})$ = 0.0023	$m(\{\theta_2\})$ = 0.0009	$m(\{\theta_2\})$ = 0.0005
	$m(\{\theta_3\})$ = 0.6379	$m(\{\theta_3\})$ = 0.0794	$m(\{\theta_3\})$ = 0.0827	$m(\{\theta_3\})$ = 0.2480	$m(\{\theta_3\})$ = 0.4160
Method in Ref. [8]	$m(\{\theta_1\})$ = 0.5529	$m(\{\theta_1\})$ = 0.9653	$m(\{\theta_1\})$ = 0.4567	$m(\{\theta_1\})$ = 0.1727	$m(\{\theta_1\})$ = 0.1442
	$m(\{\theta_2\})$ = 0.2850	$m(\{\theta_2\})$ = 0.0270	$m(\{\theta_2\})$ = 0.0673	$m(\{\theta_2\})$ = 0.0520	$m(\{\theta_2\})$ = 0.0815
	$m(\{\theta_3\})$ = 0.1621	$m(\{\theta_3\})$ = 0.0077	$m(\{\theta_3\})$ = 0.4760	$m(\{\theta_3\})$ = 0.7753	$m(\{\theta_3\})$ = 0.7743
Method in Ref. [16]	$m(\{\theta_1\})$ = 0.2322	$m(\{\theta_1\})$ = 0.9414	$m(\{\theta_1\})$ = 0.6570	$m(\{\theta_1\})$ = 0.4241	$m(\{\theta_1\})$ = 0.2903
	$m(\{\theta_2\})$ = 0.1299	$m(\{\theta_2\})$ = 0.0168	$m(\{\theta_2\})$ = 0.0360	$m(\{\theta_2\})$ = 0.0445	$m(\{\theta_2\})$ = 0.1275
	$m(\{\theta_3\})$ = 0.6379	$m(\{\theta_3\})$ = 0.0418	$m(\{\theta_3\})$ = 0.1466	$m(\{\theta_3\})$ = 0.3610	$m(\{\theta_3\})$ = 0.5823
	$m(\{\Theta\})$ = 0	$m(\{\Theta\})$ = 0	$m(\{\Theta\})$ = 0.1604	$m(\{\Theta\})$ = 0.1704	$m(\{\Theta\})$ = 0
Method in Ref. [12]	$m(\{\theta_1\})$ = 0.5529	$m(\{\theta_1\})$ = 0.9760	$m(\{\theta_1\})$ = 0.6845	$m(\{\theta_1\})$ = 0.2324	$m(\{\theta_1\})$ = 0.1982
	$m(\{\theta_2\})$ = 0.2850	$m(\{\theta_2\})$ = 0.0200	$m(\{\theta_2\})$ = 0.0383	$m(\{\theta_2\})$ = 0.0497	$m(\{\theta_2\})$ = 0.1253
	$m(\{\theta_3\})$ = 0.1621	$m(\{\theta_3\})$ = 0.0040	$m(\{\theta_3\})$ = 0.2772	$m(\{\theta_3\})$ = 0.7178	$m(\{\theta_3\})$ = 0.6765
Proposed method	$m(\{\theta_1\})$ = 0.1017	$m(\{\theta_1\})$ = 0.9562	$m(\{\theta_1\})$ = 0.3580	$m(\{\theta_1\})$ = 0.1483	$m(\{\theta_1\})$ = 0.1383
	$m(\{\theta_2\})$ = 0.0728	$m(\{\theta_2\})$ = 0.0074	$m(\{\theta_2\})$ = 0.0911	$m(\{\theta_2\})$ = 0.0469	$m(\{\theta_2\})$ = 0.0761
	$m(\{\theta_3\})$ = 0.8256	$m(\{\theta_3\})$ = 0.0364	$m(\{\theta_3\})$ = 0.5509	$m(\{\theta_3\})$ = 0.8048	$m(\{\theta_3\})$ = 0.7856

References

[1] DEMPSTER A P. Upper and lower probabilities induced by a multivalued mapping[J]. The Annals of Mathematical Statistics, 1967, 38(2): 325-339.

[2] SHAFER G. A mathematical theory of evidence[M]. London: Taylor & Francis Group, 1978.

[3] XIAO F Y. Multi-sensor data fusion based on the belief divergence measure of evidences and the belief entropy[J]. Information Fusion, 2019, 46:23-32.

[4] BAI S S, LI L J, CHEN X Y. Conflicting evidence combination based on Belief Mover's Distance[J]. Journal of Intelligent & Fuzzy Systems, 2022, 42(3): 2005-2021.

[5] HONG L, LYNCH A. Recursive temporal-spatial information fusion with applications to target identification[J]. IEEE Transactions on Aerospace and Electronic Systems, 1993, 29(2): 435-445.

[6] ZHAO Z, WU X F. Multi-points parallel information fusion for target recognition of multi-sensors[J]. Command Control and Simulation, 2020, 42(2): 23-27. (In Chinese)

[7] WU B, YI X. Research on the combination method of temporal conflict evidence based on transition matrix[J]. Mathematical Problems in Engineering, 2020, 4370613: 1-10.

[8] SONG Y F, WANG X D, LEI L, et al. Credibility decay model in temporal evidence combination[J]. Information Processing Letters, 2015, 115(2): 248-252.

[9] LUO C K, CHEN Y X, XIANG H C, et al. Evidence combination method in time domain based on reliability

and importance[J]. Journal of Systems Engineering and Electronics, 2018, 29(6): 1308-1316.

[10] WANG B, JIA J Y, DENG Z H, et al. A state monitoring method of gas regulator station based on evidence theory driven by time-domain information [J]. IEEE Transactions on Industrial Electronics, 2022, 69 (1): 694-702.

[11] LI X F, SONG Y F, LI X N. Temporal evidence fusion method with consideration of time sequence preference of decision maker[J]. Journal of Computer Applications, 2019, 39(6): 1626-1631. (In Chinese)

[12] LIU G, XIAO F Y. Time series data fusion based on evidence theory and OWA operator[J]. Sensors, 2019, 19 (5):1171.

[13] LIU G, XIAO F Y. A data-driven dynamic data fusion method based on visibility graph and evidence theory[J]. IEEE Access, 2019, 7: 104443-104452.

[14] PENG Y, HU Z H, SHEN H R. A modified distance of evidence [J]. Journal of Electronics and Information Technology, 2013, 35(7): 1624-1629. (In Chinese)

[15] DENG Y. Deng entropy[J]. Chaos, Solitons and Fractals, 2016, 91: 549-553.

[16] FAN C L, SONG Y F, LEI L, et al. Evidence reasoning for temporal uncertain information based on relative reliability evaluation[J]. Expert Systems with Applications, 2018, 113: 264-276.

HU Zhentao, born in 1979. He received his Ph. D degree in Control Science and Engineering from Northwestern Polytechnical University in 2010. He also received his B. S. and M. S. degrees from Henan University in 2003 and 2006 respectively. Now, he is a professor of School of Artificial Intelligence, Henan University. His research interests include complex system modeling and estimation, target tracking and nonlinear filter, etc.